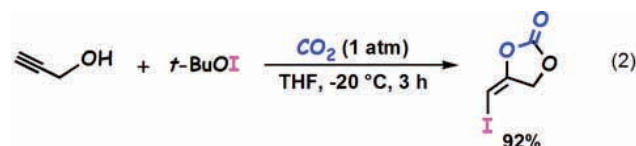


Fig.1 CO₂ fixation with (homo)allyl alcohols and *t*-BuOI.

CO₂ Fixation with Acetylenic Alcohols

The successful transformation of allyl and homoallyl alcohols to cyclic carbonates through CO₂ fixation under extremely mild conditions prompted us to investigate the use of acetylenic alcohols as substrates (Figure 2). An unsubstituted propargyl alcohol was subjected to the above CO₂ fixation reaction to afford a five-membered cyclic carbonate containing an iodomethylene group in high yield as a sole *E*-isomer (equation 2).



Propargyl alcohols having a variety of substituents at the propargylic position also trapped CO₂ to give the corresponding carbonates. Internal acetylenic alcohols were employed in the reaction, giving cyclic carbonates containing a tetrasubstituted olefin moiety. It is noteworthy that a silyl group directly attached to an acetylenic carbon resulted in a highly efficient reaction. Butynyl alcohols were also applicable to the reaction, yielding six-membered cyclic carbonates. Substituents at the propargylic position are required for the fixation of CO₂ to propargyl alcohols in conventional methods [5]. However, such substrates could be readily employed in the present system.

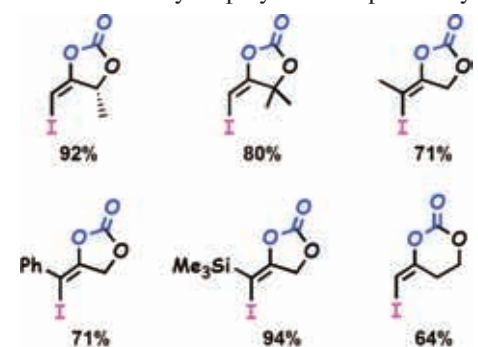
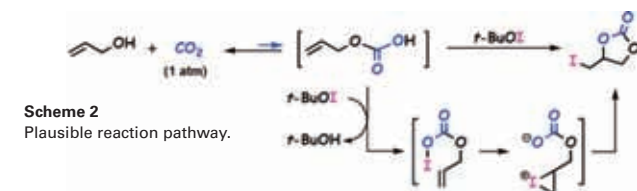


Fig.2 CO₂ fixation with acetylenic alcohols and *t*-BuOI.

Proposed Mechanism

Although the precise mechanism of the reaction is unclear at present, the proposed mechanism shown in Scheme 2 is supported by the following experimental findings. In the reaction,

t-BuOCl is added to a solution of the alcohol and NaI under an atmosphere of CO₂. NMR spectra indicated that *t*-BuOCl did not react with either the alcohol or CO₂ under these conditions. Thus, it is likely that *t*-BuOCl reacts rapidly with NaI, leading to the production of *t*-BuOI. Thus, the question arises as to which two reagents of the three present (an saturated alcohol, *t*-BuOI and CO₂) reacts first. To address this, the reaction of allyl alcohol and *t*-BuOI was monitored by ¹H NMR, and small signals, assigned to H₂C=CHCH₂OI was observed (most of the starting allyl alcohol remained unreacted). The *O*-iodinated allyl alcohol could be considered as an active intermediate, so the species prepared from the reaction of sodium allyloxide and I₂ was exposed to CO₂, but the desired reaction did not occur. Instead, the formation of acrolein was observed. In fact, when the efficiency of the reaction is less than ideal, the corresponding oxidation product, an α,β-unsaturated aldehyde was obtained. The reaction of *t*-BuOI and CO₂ was then monitored by means of NMR (¹H and ¹³C), IR and ESIMS, but no reaction was observed. Therefore, as expected initially, CO₂ fixation appears to proceed through an allyl carbonic acid intermediate, as shown in Scheme 2. The very low concentration of allyl carbonic acid would react with *t*-BuOI, leading to an *O*-iodinated species, which acts as an iodonium source and a cyclic iodonium intermediate is formed by reaction with carbon-carbon unsaturated moieties. The generation of a cyclic iodonium intermediate explains the complete stereoselectivity observed in these reactions.



Scheme 2
Plausible reaction pathway.

Conclusion

From the results of the present study and on the basis of the proposed main reaction pathway, a non-metal, non-basic, non-pressurized method was achieved, representing a new, low energy process for the chemical fixation of CO₂. The simple methodology has a very broad scope in terms of both olefinic and acetylenic alcohols, thus allowing access to a wide range of cyclic carbonates. Moreover, iodo substituents attached to sp³ and sp² carbons are versatile functional groups for organic synthesis. We conclude that the results described herein describe an innovative CO₂ fixation process that involves simple and convenient chemical manipulation and proceeds under extremely mild conditions.

References

- [1] T. Sakakura, J.-C. Choi, H. Yasuda, *Chem. Rev.* **107**, 2365 (2007).
- [2] P. G. Jessop, B. Subramaniam, *Chem. Rev.* **107**, 2666 (2007).
- [3] K. N. West, C. Wheeler, J. P. McCarney, K. N. Griffith, D. Bush, C. L. Liotta, C. A. Eckert, *J. Phys. Chem. A* **105**, 3947 (2001).
- [4] S. Minakata, Y. Morino, Y. Oderaotoshi, M. Komatsu, *Org. Lett.* **8**, 3335 (2006), S. Minakata, *Acc. Chem. Res.* **42**, 1172 (2009).
- [5] W. Yamada, Y. Sugawara, H. M. Cheng, T. Ikeno, T. Yamada, *Eur. J. Org. Chem.* 2604 (2007), Y. Kayaki, M. Yamamoto, T. Ikariya, *Angew. Chem. Int. Ed.* **48**, 4194 (2007).

Selective Growth of Monoclinic and Tetragonal Zirconia Nanocrystals

Paper in journals : this is the first page of a paper published in *Journal of the American Chemical Society*.
[*Journal of the American Chemical Society*] **132**, 2538-2539 (2010)

J|A|C|S
COMMUNICATIONS
Published on Web 02/03/2010

Selective Growth of Monoclinic and Tetragonal Zirconia Nanocrystals
Kazuyoshi Sato,* Hiroya Abe, and Satoshi Ohara
Joining and Welding Research Institute, Osaka University, 11-1 Mihogaoka, Ibaraki, Osaka 567-0047 Japan
Received December 19, 2009; E-mail: k-sato@jwri.osaka-u.ac.jp

In this communication, we demonstrate for the first time a selective growth of single-crystalline pure monoclinic and tetragonal ZrO₂ nanocrystals of <10 nm diameter, driven by controlling their surface energy. The growth of metal oxide nanocrystals with a well-organized crystalline phase is of fundamental and technological interest because in this way it is possible to tune their size-dependent unique properties,^{1,2} and thus establish their potential application in chemistry, electronics, optics, magnetics, and mechanics. ZrO₂ is a case in point, with a phase-dependent potential application in a number of technologies. Monoclinic ZrO₂ is important for catalysis,³ gate dielectrics,⁴ and bioactive coatings on bone implants,⁵ while tetragonal and cubic ZrO₂ are promising candidates for fuel cell electrolytes,⁶ oxygen sensors,⁷ and phase-transformation-toughened structural materials.⁸

In particular, the growth of pure monoclinic ZrO₂ nanocrystals of <10 nm diameter is a challenging task in the selective growth of the different phases, since a high-temperature tetragonal phase is stable at room temperature as the consequence of the dominance of the surface energy contribution to the Gibbs free energy of formation in this size range.⁹ A report by Zhang et al. suggests that the surface energy of oxides can be controlled by capping the surface with an organic substance.¹⁰ They successfully grow the unstable (001) faceted CeO₂ by capping with decanoic acid. Although surface capping-assisted growth using similar anionic substances was also applied to ZrO₂, the resulting nanocrystals of <10 nm diameter still chiefly exhibited a tetragonal phase.^{11,12} Herein, we report the facile selective growth route of pure monoclinic and tetragonal ZrO₂ nanocrystals of <10 nm diameter, with and without a cationic capping agent, N(CH₃)₄⁺.

In a typical procedure, a Zr⁴⁺ precursor (ZrOCl₂·8H₂O, 0.01 mol) was dissolved in a basic aqueous solution (pH ≈ 10.5) containing a mixture of either N(CH₃)₄HCO₃ (tetramethyl-ammonium hydrogen carbonate; TMAHC)/N(CH₃)₄OH (tetramethyl-ammonium hydroxide; TMAH) or KHCO₃/KOH. The clear solution of dissolved precursor was transferred into a 50 mL Teflon-lined, stainless steel autoclave and heat treated at 150 °C. The products were obtained as well-dispersed colloidal solutions. ZrO₂ nanocrystals in the solution were purified by washing ten times with deionized water using ultrafiltration, with a molecular weight cutoff of 3000 for subsequent characterizations. The yield of ZrO₂ nanocrystals was almost 100% in both TMAHC/TMAH and KHCO₃/KOH systems. The ZrO₂ nanocrystals were characterized by transmission electron microscopy (TEM; JEOL JEM-2100F) with an accelerating voltage of 200 kV, X-ray diffraction (XRD; JEOL JDX-3530M) with Cu Kα radiation (λ = 0.154178 nm) at 40 kV and 40 mA, Raman spectroscopy (Horiba Jobin Yvon LabRAM ARAMIS) at room temperature with 532 nm excitation line of a diode-pumped solid state laser, and UV-vis adsorption spectroscopy (Shimadzu, UV-2450) with a double-beam recording spectrometer using 1 cm quartz cells.

Figure 1 shows TEM images of ZrO₂ nanocrystals grown in the TMAHC/TMAH and KHCO₃/KOH systems. These images clearly indicate that both nanocrystals consist entirely of crystals of a uniform size of <10 nm diameter. The inset shows the high-resolution TEM (HRTEM) image of an isolated nanocrystal, indicating the single-crystalline nature of the nanocrystals grown in both systems. The lattice spacing is 0.315 and 0.295 nm, corresponding to (-111) of monoclinic and (111) of tetragonal ZrO₂ for the nanocrystals grown in the TMAHC/TMAH and the KHCO₃/KOH systems, respectively. Figure S-1 (Supporting Information) shows the size distribution of the ZrO₂ nanocrystals in the aqueous solution measured by dynamic light-scattering method, showing the nanocrystals almost perfectly dispersed in the aqueous solution by taking into account that the hydrodynamic diameter overestimates by several nanometers the real size.¹³

The XRD patterns of the powdered nanocrystals shown in Figure 2 further confirm that the respective phases observed in the HRTEM images represent the entire nanocrystals in both systems. The peaks are relatively broad, supporting the very small crystalline size. The sizes estimated by Scherrer's formula using full width of half maxima of (-111) for monoclinic and (111) for tetragonal phases were almost the same at 5.4 and 5.2 nm, respectively. The inset of Figure 2 shows the Raman spectra recorded for colloidal solutions of ZrO₂ nanocrystals. For the nanocrystals grown in the TMAHC/TMAH system, the purely monoclinic structure is confirmed by the observation of 13 Raman modes of the 18 (9A_g + 9B_g) expected by symmetry analysis,¹⁴ which provides evidence that the growth of monoclinic ZrO₂ nanocrystals shown above was driven by the surface capping with N(CH₃)₄⁺ (denoted as TMA⁺ in the following text), and not by the surface energy reduction through agglomeration by drying. The broad Raman band for the tetragonal ZrO₂ nanocrystals indicates that they involve highly disordered lattice defects.¹⁴

Optical absorption spectra of the colloidal ZrO₂ solutions shown in Figure 3 provide information relating to the lattice defects. Two absorption shoulders are clearly observed at around 5.2 and 5.7 eV for the ZrO₂ nanocrystals grown in the TMAHC/TMAH system. These are almost identical to the optical band gaps of bulk monoclinic ZrO₂,¹⁵ indicating less defective lattices.¹⁶ The tetrago-

2538 • J. AM. CHEM. SOC. 2010, 132, 2538-2539
10.1021/ja910712r © 2010 American Chemical Society

▲Reprinted with permission from *Journal of the American Chemical Society*, 2010, 132, 2538-2539. Copyright 2010 American Chemical Society.

The following is a comment on the published paper shown on the preceding page.

Selective Growth of Monoclinic and Tetragonal Zirconia Nanocrystals

SATO Kazuyoshi and OHARA Satoshi

(Joining and Welding Research Institute)

Introduction

In this communication, we demonstrate for the first time a selective growth of single-crystalline pure monoclinic and tetragonal ZrO₂ nanocrystals of < 10 nm diameter, driven by controlling their surface energy. The growth of metal oxide nanocrystals with a well organized crystalline phase is of fundamental and technological interests because in this way it is possible to tune their size-dependent unique properties,¹ and thus establish their potential application in chemistry, electronics, optics, magnetics, and mechanics. ZrO₂ is a case in point, with a phase-dependent potential application in a number of technologies.²⁻⁴

In particular, the growth of pure monoclinic ZrO₂ nanocrystals of < 10 nm diameter is a challenging task in the selective growth of the different phases, since a high-temperature tetragonal phase is stable at room temperature as the consequence of the dominance of the surface energy contribution to the Gibbs free energy of formation in this size range.⁵ A report by Zhang *et al.* suggests that the surface energy of oxides can be controlled by capping the surface with an organic substance.⁶ They successfully grow the unstable (001) faceted CeO₂ by capping with decanoic acid. Although surface capping-assisted growth using similar anionic substances was also applied to ZrO₂, the resulting nanocrystals of < 10 nm diameter still chiefly exhibited a tetragonal phase.⁷ Herein, we report the facile selective growth route of pure monoclinic and tetragonal ZrO₂ nanocrystals of < 10 nm diameter, with and without a cationic capping agent, N(CH₃)₄⁺.

Experimental procedure

In a typical procedure, a Zr⁴⁺ precursor (ZrOCl₂·8H₂O, 0.01 mol) was dissolved in a basic aqueous solution (pH ~10.5) containing a mixture of either N(CH₃)₄HCO₃ (Tetramethylammonium hydrogen carbonate; TMAHC) /N(CH₃)₄OH (Tetramethylammonium hydroxide; TMAH) or KHCO₃/KOH. The clear solution of dissolved precursor was transferred into a 50 mL, Teflon-lined stainless steel autoclave and heat treated at 150 °C. The products were obtained as well-dispersed colloidal solutions. ZrO₂ nanocrystals in the solution were purified by washing ten times with deionized water using ultrafiltration, with a molecular weight cutoff of 3000 for subsequent characterizations. The yield of ZrO₂ nanocrystals was almost 100% in both TMAHC/TMAH and KHCO₃/KOH systems. The ZrO₂ nanocrystals were characterized by transmission electron microscopy (TEM) with an accelerating voltage of 200 kV, X-ray diffraction (XRD) with Cu- α radiation ($\lambda=0.154178$ nm) at 40

kV and 40 mA, Raman spectroscopy at room temperature with 532 nm excitation line of an diode-pumped solid state laser, and UV-Vis adsorption spectroscopy with a double-beam recording spectrometer using 1 cm quartz cells.

Results and discussion

Figure 1 shows TEM images of ZrO₂ nanocrystals grown in the TMAHC/TMAH and KHCO₃/KOH systems. These images clearly indicate that both nanocrystals consist entirely of crystals of a uniform size of < 10 nm diameter. The inset shows the high-resolution TEM (HRTEM) image of an isolated nanocrystal, indicating the single-crystalline nature of the nanocrystals grown in both systems. The lattice spacing is 0.315 and 0.295 nm, corresponding to (-111) of monoclinic and (111) of tetragonal ZrO₂ for the nanocrystals grown in the TMAHC/TMAH and the KHCO₃/KOH systems, respectively. The size distribution of the ZrO₂ nanocrystals in the aqueous solution measured by dynamic light-scattering method (not shown here) indicates that the nanocrystals almost perfectly dispersed in the aqueous solution.

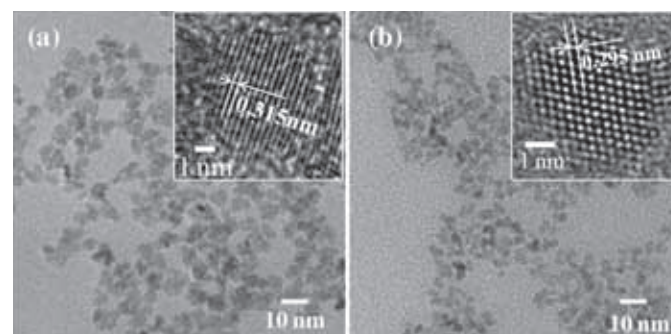


Fig.1 TEM images of ZrO₂ nanocrystals grown in the (a) TMAHC/TMAH and the (b) KHCO₃/KOH systems. The inset shows HRTEM image of an isolated nanocrystals.

The XRD patterns of the powdered nanocrystals shown in Figure 2 further confirm that the respective phases observed in the HRTEM images represent the entire nanocrystals in both systems. The peaks are relatively broad, supporting the very small crystalline size. The sizes estimated by Scherrer's formula using full width of half maxima of (-111) for monoclinic and (111) for tetragonal phases were almost the same at 5.4 and 5.2 nm, respectively. The inset of Figure 2 shows the Raman spectra recorded for colloidal solutions of ZrO₂ nanocrystals. For the nanocrystals grown in the TMAHC/TMAH system, the purely monoclinic structure is confirmed by the observation of 13 Raman modes of the 18 (9A_{1g} + 9B_{1g}) expected by symmetry analysis,⁸ which provides evidence that the growth of monoclinic ZrO₂ nanocrystals shown above was driven by the surface

capping with N(CH₃)₄⁺ (denoted as TMA⁺ in the following text), and not by the surface energy reduction through agglomeration by drying. The broad Raman band for the tetragonal ZrO₂ nanocrystals indicates that they involve highly disordered lattice defects.⁸

Optical absorption spectra of the colloidal ZrO₂ solutions shown in Figure 3 provide information relating to the lattice defects. Two absorption shoulders are clearly observed at around 5.2 and 5.7 eV for the ZrO₂ nanocrystals grown in the TMAHC/TMAH system. These are almost identical to the optical band gap of bulk monoclinic ZrO₂,⁹ indicating less defective lattices.¹⁰ The tetragonal ZrO₂ showed only one absorption shoulder at a lower photon energy (approximately at 5.1 eV) than those of monoclinic ZrO₂, indicating the presence of many lattice defects, probably cation impurity and/or oxygen vacancy.⁸ Inductively coupled plasma atomic emission spectroscopy revealed that the concentration of K⁺ in the tetragonal ZrO₂ was negligible (<10⁻⁷ mol · g⁻¹). Thus, it can be concluded that the major lattice defects in the tetragonal ZrO₂ are oxygen vacancies, which is consistent with a previous report.¹⁰

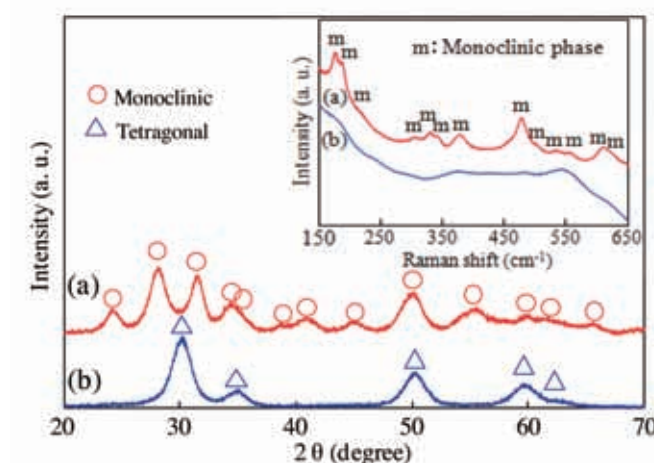


Fig.2 XRD profiles of ZrO₂ nanocrystals grown in the (a) TMAHC/TMAH and the (b) KHCO₃/KOH systems. The inset shows Raman spectra of colloidal solutions of ZrO₂ nanocrystals grown in the (a) TMAHC/TMAH and the (b) KHCO₃/KOH systems.

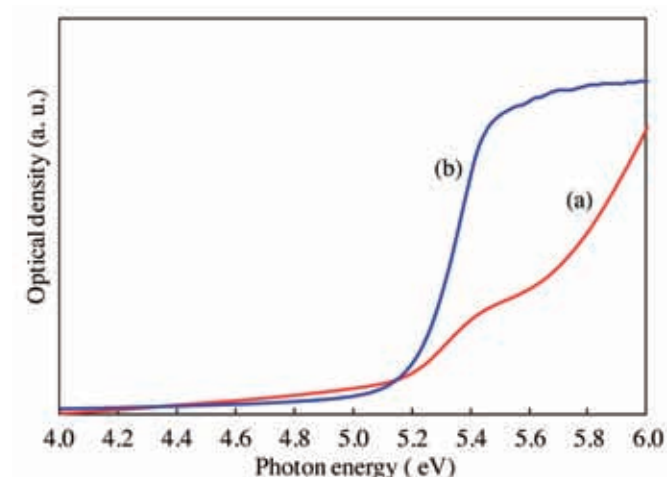


Fig.3 Optical absorption spectra of colloidal solutions of ZrO₂ nanocrystals grown in the (a) TMAHC/TMAH and the (b) KHCO₃/KOH systems.

Here we discuss how the selective growth of monoclinic and tetragonal ZrO₂ nanocrystals was achieved. Monoclinic ZrO₂ nanocrystals may be formed due to the reduction of surface energy through capping with TMA⁺, since the capping with organic substances has the potential to reduce the surface energy of oxides by more than 1.7 J·m⁻² compared with bare surface as suggested by the literature,^{6,11} while the surface energy of monoclinic ZrO₂ is only approximately 0.4 J·m⁻² higher than that of tetragonal.⁵ The differential thermal analysis showed that TMA⁺ persists on the nanocrystals up to 280 °C. The considerably higher temperature than the vaporization temperature of free TMAH (157 °C) indicates that TMA⁺ successfully caps the surface of ZrO₂ nanocrystals. By contrast, the absence of K⁺ in the ZrO₂ grown in the KHCO₃/KOH system as shown above indicates that the K⁺ does not cap the nanocrystals; thereby, the tetragonal phase is spontaneously formed.⁴

It is suggested that the energy state of surface oxygen plays a vital role in the size-dependent phase stability of ZrO₂ nanocrystals, since the stable phase strongly depends on the sign of charge of the capping agent, i.e., monoclinic ZrO₂ is obtained when the negatively charged surface oxygen is capped with oppositely charged TMA⁺. By contrast, the tetragonal phase is stabilized when the nanocrystals are capped with anionic substances,⁷ in which the surface oxygen may be exposed to the surrounding medium the same as in the case of uncapped nanocrystals (KHCO₃/KOH system in this study). The oxygen vacancies in the tetragonal ZrO₂ may be formed as a consequence of relaxation of the unstable surface oxygen.

Conclusion

The present study offers a simple approach for the selective growth of pure monoclinic and tetragonal ZrO₂ nanocrystals of < 10 nm diameter capped with and without TMA⁺, respectively. The present concept, surface energy control via the capping with an adequate agent, may be a promising universal approach to control the crystal phase of technologically important oxide nanocrystals such as Al₂O₃, TiO₂, BaTiO₃, and PbTiO₃, consequently enabling us to tune their unique properties.

References

- [1] Garcia-Barriocanal, J.; Rivera-Calzada, A.; Varela, M.; Sefrioui, Z.; Iborra, E.; Leon, E.; Pennycook, J.; Santamaria, J. *Science* **2008**, *321*, 676.
- [2] He, D.; Ding, Y.; Luo, H.; Li, C. *J. Molec. Catal.* **2004**, *208*, 267.
- [3] Shin, J. H.; Chao, C.-C.; Huang, H.; Prinz, F. B. *Chem. Mater.* **2007**, *19*, 3850.
- [4] Garvie, R. C.; Hannink, R. H.; Pascoe, R. T. *Nature* **1975**, *258*, 703.
- [5] Garvie, R. C. *J. Phys. Chem.*, **1978**, *82*, 218.
- [6] Zhang, J.; Ohara, S.; Umetsu, M.; Naka, T.; Hatakeyama, Y.; Adschiri, T. *Adv. Mater.*, **2007**, *19*, 203.
- [7] Zhao, N.; Pan, D.; Nie W.; Ji, X., *J. Am. Chem. Soc.*, **2006**, *128*, 10118.
- [8] Michel, D.; Perez, M.; Jorba, Y.; Collongues, R. J. *Raman Spectrosc.*, **1976**, *5*, 163.
- [9] Kwok, C.-K.; Aita, C. R. *J. Appl. Phys.*, **1989**, *66*, 2756.
- [10] Yashima, M.; Tsunekawa, S.; *Acta Cryst.*, **2006**, *B62*, 161.
- [11] Conesa, J. C. *Surface. Sci.*, **1995**, *339*, 337.